



## A Simplified Approach to Calculate Particle Growth Rate Due to Self-Coagulation, Scavenging and Condensation Using SMPS Measurements during a Particle Growth Event in New Delhi

Bighnaraj Sarangi, Shankar G. Aggarwal<sup>\*</sup>, Prabhat K. Gupta

CSIR-National Physical Laboratory, Dr. K. S. Krishnan Marg, New Delhi 110012, India

---

### ABSTRACT

The scanning mobility particle sizer (SMPS) technique is a widely employed technique to measure the particle number size distribution, and thus calculate the particle total growth rate. However, growth due to individual atmospheric processes needs to be known precisely and accurately to better model the secondary aerosol distribution. In this study, we use simplified analytical formulas to calculate the growth rates due to self-coagulation, coagulation scavenging and condensation processes of particle size distribution (9–425 nm) measured using SMPS. Firstly, total growth rate is determined from the regression fit of SMPS data plotted between the geometric mean diameter (GMD) of particle size (nm) versus time (hour) measured during a particle growth event. The SMPS measurements were conducted during November–December 2011 in New Delhi. The particle growth event days and non-event days were classified according to the protocol discussed elsewhere. Assuming that the particle number size distribution of a growing population can be described by a unimodal distribution and particles are neutral in the population, we calculated the growth rate due to self-coagulation ( $GR_{\text{scog}}$ ), which is proportional to the total number of particles in the mode and mode peak diameter. Similarly, assuming that particles with mode peak size 25 nm and above act as a coagulation sink and grow due to scavenging of newly formed nucleation range particles (< 12 nm), we calculated the coagulation scavenging growth rate ( $GR_{\text{scav}}$ ) as a time derivative of the mode peak diameter, which is equivalent to the product of particle diameter and its coagulation sink. The condensation growth rate ( $GR_{\text{cond}}$ ) is calculated based on the assumption that total growth rate is the summation of the growth resulting of three physical processes: self-coagulation, coagulation scavenging and condensation. During the study period, three event days were recorded at the measurement site. To explain the growth rate calculation approach, which is presented here in detail, we have taken SMPS data of one event day (November 4, 2011) as an example (two other event days are also briefly discussed). On November 4, the total average growth rate was found to be  $15.4 \pm 11$  nm/h, while the average  $GR_{\text{scog}}$ ,  $GR_{\text{scav}}$  and  $GR_{\text{cond}}$  were calculated to be  $3.8 \pm 0.4$  (with min and max values of 2.9–5.1 nm/h),  $8.0 \pm 6$  (0.6–19.3 nm/h) and 3.6 nm/h, respectively. These growth rates are comparable to those reported for other urban sites around the world using different methods. This approach is simple, and growth by individual processes can be calculated without knowing several other parameters, which include vapor concentration of atmospheric constituents, heterogeneous processes, and complex modeling procedures.

**Keywords:** SMPS measurements; Particle growth rate calculations; Self-coagulation; Coagulation scavenging and Condensation growth.

---

### INTRODUCTION

Secondary aerosols are formed from transformation of atmospheric gas-phase species to the particulate matter (PM) whose contribution is important in total aerosol mass in many urban and remote areas (Finlayson-Pitts and Pitts Jr., 2000; Kulmala *et al.*, 2013; Seinfeld and Pandis, 2006). Understanding the effects of secondary aerosols on climate

and health are more complex as their distribution and fraction in total aerosol mass are highly uncertain. Particle formation and growth have been observed in several places on the globe (Kulmala *et al.*, 2001, 2004; Bzdek and Johnston, 2010). Measurement of frequency of these nucleation events and subsequent particle growth can help to better constrain the secondary aerosols distribution, and hence aerosol effects (Kulmala *et al.*, 2013).

The newly formed aerosols become climatically important only if they are able to grow to sizes of 50 nm and larger. Particles in this size range can act as cloud condensation nuclei (Twomey 1974; Pirjola *et al.*, 2002; Laaksonen *et al.*, 2005; Kaufman *et al.*, 2006) and they contribute to

---

<sup>\*</sup> Corresponding author.

E-mail address: aggarwalsg@nplindia.org

indirect aerosol effect on the climate (Lehtinen and Kulmala, 2003). Furthermore, if the particles grow to sizes above about 100 nm, they scatter light very efficiently, and have thereby a direct (cooling) effect on the Earth climate (Coakley, 2005). Due to their Brownian motion, particles with diameter of about 10 nm coagulate very efficiently with larger particles, which implies that the freshly nucleated particles grow fairly rapidly (within a few hours) cross the 10 nm limit or in other words, they get lost in the collision processes (Kulmala *et al.*, 2000). In order to determine the causes of atmospheric nucleation events, and to better understand the characteristic of these events in different environments, it is important to know the underlying processes causing the particle growth and the physiochemical mechanisms controlling their formation and growth processes.

Several methods have been developed for determining aerosols growth rates from atmospheric observations. They are derived through complex mathematical equations, which rely on particle number size distribution measurements. To estimate aerosol growth rate accurately, models must include microphysical processes such as nucleation, coagulation, scavenging, condensation/evaporation, etc. However, calculation of growth rates due to these processes are not so straightforward and needs to know several information, such as nucleation range particle with size, number and charge; vapor concentration of atmospheric constituents, and heterogeneous processes, etc. Moreover to collect this information, innovative instrumental techniques are needed.

Depending upon the atmospheric conditions, aerosol particles grow mainly due to both condensation and coagulation (Dal Maso *et al.*, 2005; Leppä *et al.*, 2011). Condensation growth is considered as condensation of vapors onto pre-existing particles. In these conditions the growth rate depends on the particle diameter only through the Kelvin effect (i.e., equilibrium vapors pressure over a curved surface (Seinfeld and Pandis, 2006)).

Coagulation is a kinetic process in which particles those are in relative motion, collide and fuse. In this process, the effect of particle charge is a dominant factor for small particles (Fuchs, 1964). There are two types of coagulation processes discussed in general, (i) self-coagulation, which is defined as fusion of similar sized particles, and (ii) coagulation scavenging, which is referred as scavenging of freshly form nucleation range particles by the pre-existing relatively bigger sized particles.

The atmosphere of several megacities are reported to be highly affected by anthropogenic emissions and dense industrial plumes (Butler *et al.*, 2011), where coagulation plays a key role in the removal of aerosols because of the high concentration of particles, and on the other hand due to formation of new particles. To simulate changes in the size distribution of coagulating aerosols, modelers and researchers have developed a number of approaches that assume either a continuous size spectrum or discrete bins that vary in sizes (Turco *et al.*, 1979; Kim and Seinfeld, 1990). Turco *et al.* (1979) derived a basic semi-implicit algorithm to describe aerosol coagulation with an assumed geometrically related size distribution and a volume ratio of size bins equal to two. Jacobson and Turco (1994) further

developed these coagulation equations to allow the volume ratio of the adjacent bins to approach unity and to simulate coagulation among any number of particle types, each containing any number of volume fraction components. The long-term goal of the study was to develop a microphysical model that will adequately simulate aerosol size distributions.

Simulating coagulation in a particle size growth study is important in order to decrease large particle numbers. From modeling point of view, particles self-coagulation and coagulation scavenging can be treated comfortably, whereas condensation processes are problematic because of our incomplete knowledge on the vapors participating into these processes and in general lack of knowledge of vapor properties (e.g., Nieminen *et al.*, 2010; Wang *et al.*, 2010).

In this paper, we have used a novel approach and applied the equations in a simplified form, which have been discussed in Leppä *et al.* (2011) and Seinfeld and Pandis (2006) to calculate particle growth rates using real ambient number size data. We have calculated particle growth based on the SMPS measurements in a megacity, New Delhi. The methodology mainly includes two assumptions, (i) the total growth of the particle at different modes are the summation of particle growth due to self-coagulation, coagulation scavenging and condensational processes, and (ii) while calculating growth due to coagulation scavenging, we assumed that particles in the nucleation range below 12 nm are freshly formed and being scavenged by mode particle of the distribution which grows into mode particle of the succeeding samples (size distribution). The growth rates due to these 3 individual processes are calculated for a growth event day (November 4) as an example. We also discussed here the effect of meteorological conditions on the growth of particle.

## METHODOLOGY

### *Instrumentation*

Particle size measurements were carried out at National Physical Laboratory (NPL, <http://www.nplindia.org/>), New Delhi. Fig. 1 shows a google view of the sampling location. The sampling site is surrounded largely by vegetation, residential apartments and a light traffic road. As can be seen in figure, it is a representative site of mixed source influence, such as, biomass burning, traffic emission, biogenic emission and other combustion/burning sources from residential colonies. This location and sources are discussed in details in recent publications on chemistry of aerosols collected in the same site (Miyazaki *et al.*, 2009; Li *et al.*, 2014).

The measurement system was placed in a room at the top floor of the building. The system consisted of a scanning mobility particle sizer (SMPS), which comprises an electrostatic classifier (TSI model 3080) and Kr-85 neutralizer, a differential mobility analyzer (DMA, TSI model 3081) and a condensation particle counter (CPC, TSI model 3788). Aerosol samples were aspirated at the rooftop of the laboratory (~15 m above the ground) through a cyclone inlet (2.5  $\mu\text{m}$  cutoff size) connected with stainless steel tubing of internal diameter 6 mm and length ~4 m, Fig. 2. Then aerosols were dried after passing through two



is observed. The classification is further discussed in the following section.

### Particle Growth Rate Calculation

Particle growth rates were represented by the observed growth in Atkins and accumulation ranges. The number concentration of particles at the start and end of a period during which a subsequent increase in size was observed, were used to quantify the total growth rate. Geometric mean diameters (GMD) for each size distribution were used to examine particle growth processes (Jeong *et al.*, 2010). The observed growth rate ( $GR_{total}$ ) of the ambient particle was quantified by fitting the GMD of particles in modal ranges during the growth process event over a period of time 't'.

$$GR_{total} = \frac{\Delta GMD}{\Delta t} \quad (1)$$

$$GMD(d_g) = \exp \frac{\sum_i (\ln d_{pi}) \times N_i}{\sum_i N_i} \quad (2)$$

where  $d_g$  is the geometric mean diameter of the particles,  $d_{pi}$  is the particle diameter of size bin  $i$ , and  $N_i$  is the particle number concentration in size bin  $i$  (Hinds, 1998).

We assume that aerosol particles are spherical and thus have a well-defined diameter. By growth of a single particle, we mean the increase of diameter of that particle. Particle diameter increases due to self-coagulation, coagulation scavenging and condensation, which are the only processes those considered in the growth of a single particle in our approach. Fig. 3 shows the growth of the particle due to these three processes, i.e.,

$$GR_{total} = GR_{scoag} + GR_{scav} + GR_{cond} \quad (3)$$

where  $GR_{total}$  is the total growth rate,  $GR_{scoag}$  is the growth rate due to self-coagulation (coagulation of similar size particles in the population with each other),  $GR_{scav}$  is the growth rate due to coagulation scavenging (coagulation of

smaller diameter particles in the population with pre-existing bigger sized particles),  $GR_{cond}$  is the growth rate due to condensation of vapors on the pre-existing particles in the atmosphere.

### Self-Coagulation

To estimate the growth rate due to self-coagulation, we make a simple assumption that the particle number size distribution of a growing population can be described by a unimodal distribution then growth rate due to self-coagulation (procedure described in Leppä *et al.*, 2011) can be defined as:

$$GR_{scoag}(d_p) = \frac{d_p}{6} k(d_p) N \quad (4)$$

where  $N$  is the total number concentration of particles in the mode peak, and  $k(d_p)$  is the Brownian coagulation coefficient between the particles of similar size,  $k(d_p)$  can be determined as:

$$k(d_p) = 3 \times 10^{-16} \times C_c \quad (5)$$

where  $C_c$  is known as Cunningham slip factor (Hinds, 1998).

### Coagulation Scavenging

The approach used in this study is based on the assumption that in ambient atmosphere, Atkins (25 to 100 nm) and accumulation ( $> 100$  nm) range particles act as coagulation sink for newly formed nucleation range ( $< 12$  nm) particles. The coagulation of larger particle with the newly formed particles ( $< 12$  nm) resulted as decrease in number concentration of nucleation range particles and growth of Atkins and accumulation range particles. Using particle number size distribution, the value of coagulation sink for the particles in a mode can be calculated as discussed in Leppä *et al.* (2011):

$$CoagS_i = \sum_{j=p}^q k(d_p)_{ij} \times N_j \quad (6)$$

where  $k(d_p)_{ij}$  is the Brownian coagulation coefficient

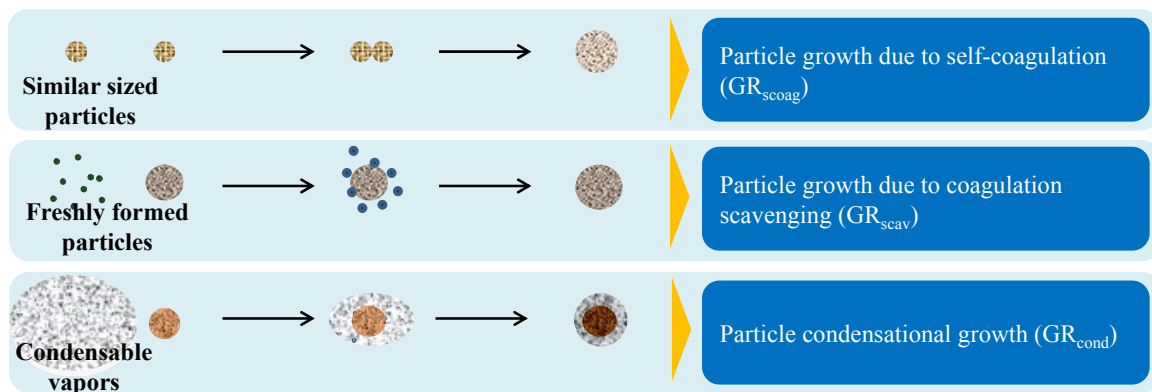


**Fig. 3.** Pictorial presentation of the processes of growth of the particle due to self-coagulation, coagulation scavenging and condensational growth.

between particles in sections  $i$  and  $j$  and particles in the nucleation range in sections from  $p$  to  $q$ . Here  $N_j$  is the nucleation range particle number concentration, which are scavenged by the larger one. Detail process is described in Fig. 4.

Fig. 4 is a simple representation of particle growth rate due to scavenging. Figure illustrates the two consecutive distributions. The distribution with blue color represents the initial particle size distribution (sample 1), and the other with red color is the succeeding size distribution (sample 2).  $d_m$  and  $d_m'$  are the mode peak of initial (preceding) and succeeding size distributions, respectively.  $N_j'$  and  $N_j''$  are the nucleation range ( $< 12$  nm in this study) particles number concentration in initial and succeeding distributions, respectively. Particles equivalent to the loss in nucleation range particle number concentration  $N_j$  ( $= N_j' - N_j''$ ) coagulate with the initial mode ( $d_m$ ), so as a result, the size (equivalent) of  $d_m$  is enhanced to  $d_m'$  in the succeeding distribution (sample 2) with the progress of time.

$$k(d_p)_{ij} = (D_i d_i + D_j d_j + D_j d_i + D_i d_j) \pi \beta \quad (7)$$

where  $D$  and  $d$  denote the diffusion coefficients and particle diameter of class  $i$  and  $j$ , respectively,  $\beta$  is the correction factor for the particles in transition and free molecular regime as suggested by Fuchs (1964).

Diffusion coefficient can be calculated as (Hinds, 1998):

$$D = \frac{kTC_c}{3\pi\eta d_p} \quad (8)$$

where  $d_p$  is the particle diameter and  $k$ ,  $T$  and  $\eta$  are the Boltzmann constant, temperature at standard condition, and coefficient of viscosity, respectively.  $C_c$  is called Cunningham slip correction factor. Eq. (8) agrees with the correlation (adjusted for mean free path,  $\lambda$ ) developed by Allen and Raabe (1985) for all particle sizes.

Leppä *et al.* (2011) derived an equation to estimate the growth rate due to scavenging as:

$$\begin{aligned} GR_{scav} &= d_{p^*} \frac{\sum_{i=1}^n CoagS_i N_i}{\sum_{i=1}^n N_i} - \frac{\sum_{i=1}^n CoagS_i N_i d_{pi}}{\sum_{i=1}^n N_i} \\ &= d_{p^*} \times CoagS^* - (d_p \times CoagS)^* \end{aligned} \quad (9)$$

where  $d_{p^*}$  is the count mean diameter,  $d_{pi}$ ,  $N_i$  and  $CoagS_i$  are the particle diameter, number concentration and coagulation sink for the particles in class  $i$ , respectively, and  $*$  denotes the count mean value over the nucleation mode. In our approach, the mode diameter in size distribution is treated as the coagulation sink for the small range particles existing in the same distribution as discussed in Fig. 4.

If  $d_m$  describes the size of the mode for number size distribution either at Atkins or accumulation range, the growth rate due to coagulation scavenging can be defined as a time derivative of that diameter:

$$GR_{scav} = \frac{dd_m}{dt} = d_m CoagS_i \quad (10)$$

Eq. (10) is the modified form of growth rate due to scavenging as discussed by Leppä *et al.* (2011).

### Condensation

Under most atmospheric conditions, aerosol particles grow mainly due to condensation of vapors on them. The growth rate of a particle diameter due to condensation is then calculated as (Seinfeld and Pandis, 2006):

$$GR_{cond} = \frac{1}{2} \times V_m \times v \times \alpha (C_\infty - C_s) \quad (11)$$

where  $V_m$  is the volume of the condensing vapor molecule,

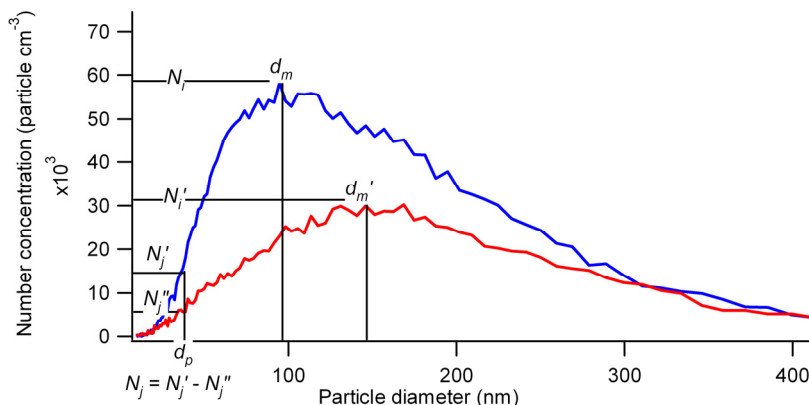


**Fig. 4.** The growth observed in mode peak ( $d_m'$ ) (in succeeding sample) as the existing nucleation range particles ( $N_j$ ) being scavenged by preceding mode peak ( $d_m$ ) in a sample. Here  $d_m'$  is always greater than  $d_m$ . Where  $d_m$  = mode particle diameter (nm),  $N_i$  = mode particle number concentration (particle/cm<sup>3</sup>),  $d_m'$  = mode diameter after growth (nm),  $N_i'$  = number concentration (particle/cm<sup>3</sup>) after growth,  $d_p$  = particle diameter in nucleation range (nm),  $N_j'$  = number concentration of the particles at nucleation range (particle/cm<sup>3</sup>),  $N_j''$  = number concentration of the particles at nucleation range after  $d_m$  grows to  $d_m'$ ,  $N_j$  = loss in nuclear range particles (particle/cm<sup>3</sup>) scavenged by  $d_m$ , which grows to  $d_m'$ .

$v$  is the mean speed of the molecules;  $C_\infty$  and  $C_s$  are the number concentration of condensing molecules far away from the particle and the saturation vapor concentration at the particle surface, respectively, and  $\alpha$  is the molecular accommodation coefficient.

### Particle Charge Effect on Growth

This is important to note that in this study, we did not account for the effect of particle charge in self-coagulation, coagulation scavenging and condensation processes. Leppä *et al.* (2011) discussed about the role of charged particles and electric interactions in the growth of nucleation mode particles. They reported that charged particles can increase the growth rate due to both self-coagulation (in < 20 nm particle range) and coagulation scavenging (by bigger particles) by a factor of 1.5 to 2. They suggested that the total condensational growth rate of a nucleation mode may increase significantly in very early steps of the growth in case of charged particles. However in the present study, we have measured particle size in the range of 9–425 nm by aiming to calculate the growth rates of these particles (for this range of particles, the distribution mode peak is observed to be in between 88–174 nm). Further, particle charge affects the growth rate of nucleation range particles, but this effect may be less significant for Atkins or accumulation range particles (Fuchs, 1964; Kerminen *et al.*, 2007), which are being studied here.

## RESULTS AND DISCUSSION

### Growth Event Days versus Non-Event Days

Based on the observed number-size distribution, days are classified in growth event and growth non-event days. The classification method of growth events that we used here is based on nucleation event methods as described by Mäkelä *et al.* (2000) and Dal Maso *et al.* (2005). A day is considered as growth event day if the growth of aerosol particles mode is observed over a period of several hours (at least for 1 hour). In practice, a new particle formation event can be seen as an increase of the particle number concentration in the smallest size bins of the SMPS system. These newly formed particles then experience subsequent growth that can be seen to occur typically at a rate of few nanometers per hour during rest of the time. If the aerosol size distribution for a given day exhibits these signs, the day is classified as a typical growth event day. Rests of the days are classified as growth non-event days, where no particle growth is observed in the mode peak of the number-size distribution. Fig. 5 presents examples of particle growth and their classification.

Particle number size distribution measurements (9–425 nm) were conducted at NPL, New Delhi for 10 days during November–December 2011. During this period, 3 growth event days (November 4, December 15 and 26) were identified, where particle growth of Atkins and accumulation

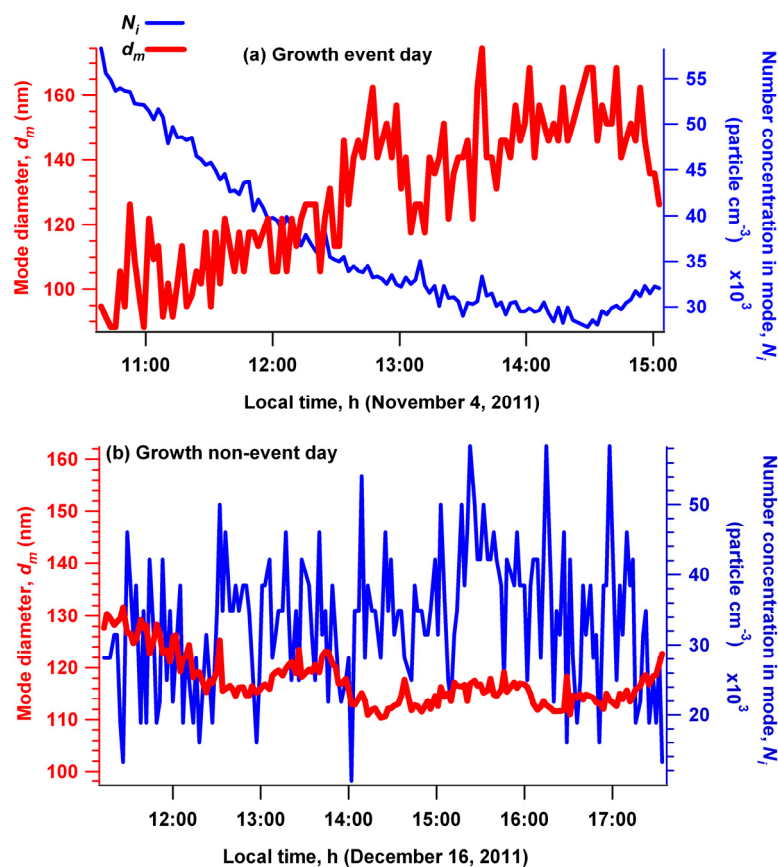


**Fig. 5.** A comparison between particle mode peak diameter and number concentration in the mode during particle growth event day (November 4) and non-event day (December 16).

range is recorded for at least 1 hour. Rest all days are classified as non-event days. For example, we observed longest growth event day for about 4 hours on November 4, while December 16 is shown as an example of growth non-event day in Fig. 5. During particle growth, a clear relation (inversely proportional) between mode peak diameter and particle number concentration in the mode peak can be seen, Fig. 5(a). Particle size in the mode peak is increased with time but on the other hand, number concentration in the mode is systematically decreased. This suggests that coagulation is a dominant process of particle growth. Similar results are also observed for other days of the growth event in this study. Different from growth event day, no regular trend between mode size and particle number concentration in mode peak was observed on December 16, Fig. 5(b). In addition, large variation in particle mode peak concentration is recorded with time on the non-event day. Consistent with the observation in Fig. 5(a), particle total number concentration is also found to decrease with particle mode size, Fig. 6. This further suggests that coagulation processes are important for particle growth which can govern the particle number and size distribution in an urban atmosphere. On the growth event day (i.e., November 4), the total particle number concentration ( $N_{\text{total}}$ ) was recorded to be varied between  $2.77 \times 10^4$  to  $5.55 \times 10^4$  particle/cm<sup>3</sup> (with an average of  $3.72 \times 10^4$  particle/cm<sup>3</sup>). On the other hand, on non-event day (i.e., December 16),  $N_{\text{total}}$  varied between  $1.96 \times 10^4$  to  $3.54 \times 10^5$  particle/cm<sup>3</sup> ( $2.49 \times 10^4$  particle/cm<sup>3</sup>).

This number concentration is comparable with the number concentration observed at Po Vally (Italy), Marikana (South Africa), Wakayama (Japan), Maxico city and Shanghai (China). In general, low number concentration have been

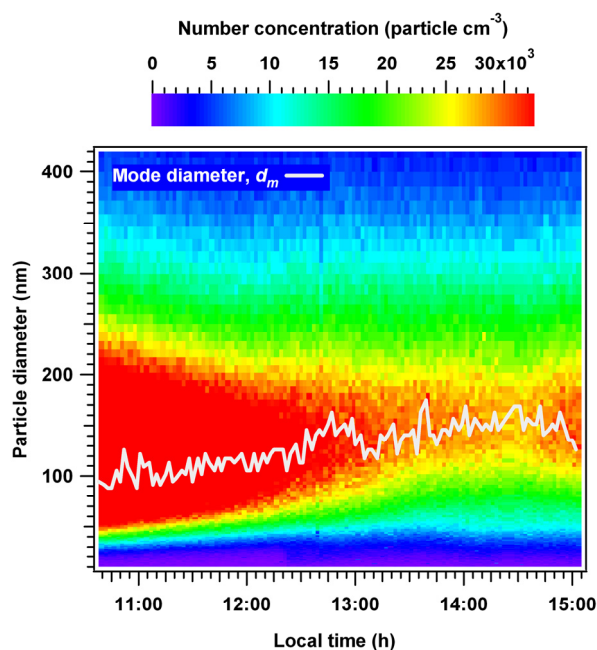


**Fig. 6.** Time series of size-resolved particle number concentration on November 4 (i.e., a growth event day). The white line represents the particle mode peak diameter.

reported for relatively less polluted (clean) sites (Komppula *et al.*, 2003; Asmi *et al.*, 2010), whereas high values have been observed for relatively more polluted areas those are affected by long-range anthropogenic transport, local traffic, industrial and biomass burning emissions (e.g., Rodriguez *et al.*, 2005; Kalafut-Pettibone *et al.*, 2011; Du *et al.*, 2012; Hirsikko *et al.*, 2012), Table 1. Observed high number concentration of particles in New Delhi atmosphere supported the high level of pollution in the megacity reported recently (Miyazaki *et al.*, 2009; Li *et al.*, 2014).

### Particle Growth Rate

Total growth rate of particles ( $GR_{\text{total}}$ ) can be estimated from the measured size distribution data. For an example, we determined the growth rate based on the SMPS data measured on a typical growth event day, i.e., on November 4. As depicted in Fig. 5(a), on this day a continuous growth for 4 hours of the particles was observed. Fig. 7 shows a plot between geometric mean diameter (GMD, nm) of particle size distribution plotted against local time (hour) during the growth event day. The growth rates for different time periods of this event day were determined by fitting of the data of a particular time segment (minimum growth time of about 1 hour) for which an abrupt change in GMD was observed (Fig. 7), especially during noontime (this point is further discussed in the following section in the context of meteorological parameters). Average growth rate was determined by fitting of total data of about 4 hours. The slope of the regression fit of the data (dotted line) gives the growth rate (nm/h) during the period.

The total growth rate from the regression fit was estimated to be  $15.4 \pm 11$  (here standard error is the error of the regression fit for the predicted growth rate). For example, this growth rate is comparable with the growth rates observed in Po Vally (Italy), Beijing (China) and Tokyo (Japan), Table 1. In general, low growth rates have been reported for relatively less polluted (clean) sites (Weber *et al.*, 1997; Birmili and Wiedensohler, 2000; Dal Maso *et al.*, 2005), whereas high values have been observed for more polluted cities those are affected by long-range anthropogenic transport, local traffic, industrial and biomass burning emissions (Birmili and Wiedensohler, 2000; Verheggen and Mozurkewich, 2002; Birmili *et al.*, 2003; Kulmala *et al.*, 2005). As discussed above, observed high particle growth rate in New Delhi atmosphere suggested that increased level of pollution in the megacity (Miyazaki *et al.*, 2009).

On November 4, the growth rate due to self-coagulation ( $GR_{\text{scog}}$ ) was calculated using Eq. (4). Average growth rate due to self-coagulation was calculated to be  $3.8 \pm 0.4$  nm/h with minimum and maximum values were 2.9 and 5.1 nm/h, respectively. Figs. 8(a) and 8(b) represent  $GR_{\text{scog}}$  versus mode size, and  $GR_{\text{scog}}$  versus local time, respectively. Fig. 8(a) shows that in general,  $GR_{\text{scog}}$  increases with mode diameter of the size distribution. However, this trend is not very clear for smaller mode diameter (i.e., < 120 nm). The  $GR_{\text{scog}}$  was found to be relatively low around 12:00 to 14:00 h (LT), Fig. 8(b). A possible reason for this is meteorological conditions, especially relative humidity and solar radiation those impact on  $GR_{\text{scog}}$ . Relative humidity

**Table 1.** Particle number concentration and growth rate observed in different locations on the globe.

| Location                                      | Particle size range (nm) | Observed/considered nucleation mode size range (nm) | Average number concentration (particle/cm <sup>3</sup> ) | Average growth Rate (nm/h) | Reference                              |
|---|--------------------------|---|--|----------------------------|--|
| Idaho Hill, Colorado                          | 15–500                   | 3–20  | $\sim 1 \times 10^4$                                     | 1.6                        | Weber <i>et al.</i> , 1997             |
| Rural Ontario, Canada                         | 11–457                   | 10–43   | $2 \times 10^4$  | 4.2                        | Verheggen and Mozurkewich, 2002        |
| Northern Finland                              | 7–500                    | 7–15  | $8.7 \times 10^2$  | 2.9                        | Komppula <i>et al.</i> , 2003          |
| Rural continental site in southern Germany    | 3–800                    | 3–20  | $\sim 5 \times 10^3$                                     | 2.6                        | Birmili <i>et al.</i> , 2003           |
| Po Valley, Italy                              | 3–20, 15–600             | 3–20  | $1.2 \times 10^4$  | 7                          | Hamed <i>et al.</i> , 2007             |
| Hyytiälä, Finland                             | 3–500                    | < 25  | —  | 3                          | Dal Maso <i>et al.</i> , 2007          |
| Tokyo, Japan                                  | 50–200                   | —   | $\sim 10^3$  | 8–17*                      | Mochida <i>et al.</i> , 2008           |
| Antarctic                                     | 3–1000                   | 3–25  | 374  | 1.3                        | Asmi <i>et al.</i> , 2010              |
| Toronto, Canada                               | 3–100                    | 14–25   | $1.05 \times 10^4$                                       | 6.7                        | Jeong <i>et al.</i> , 2010             |
| Mexico city                                   | 10–478                   | 10–15   | $2.1 \times 10^4$  | 11.6                       | Kalafut-Pettibone <i>et al.</i> , 2010 |
| Beijing, China                                | 12–550                   | 12–25   | $\sim 10^3$  | 2.43–13.9*                 | Zhang <i>et al.</i> , 2011             |
| Brisbane, Australia                           | 4–110                    | 4–30  | $5.6 \times 10^3$  | 4.6                        | Cheung <i>et al.</i> , 2011            |
| Shanghai, China                               | 10–500                   | 10–20   | $1.3 \times 10^4$  | 4.38                       | Du <i>et al.</i> , 2012                |
| Marikana, South Africa                        | 10–840                   | 12–20   | $1 \times 10^4$  | 8                          | Hirsikko <i>et al.</i> , 2012          |
| Atlanta, USA                                  | 3–500                    | $\sim 1$ –3 <sup>#</sup>                            | $10^3$ – $10^7$ *  | 5.5–7.6*                   | Kuang <i>et al.</i> , 2012             |
| Wakayama Forest Research Station, Japan       | 14–710                   | 14–30   | $1.1 \times 10^4$  | 9.2                        | Han <i>et al.</i> , 2013               |
| National Physical Laboratory (NPL), New Delhi | 9–425                    | 9–25  | $3.72 \times 10^4$                                       | 15.4                       | This study (November 4, 2011)          |

# geometric mean diameter (freshly formed nuclei).

\* growth rate range or number concentration range.

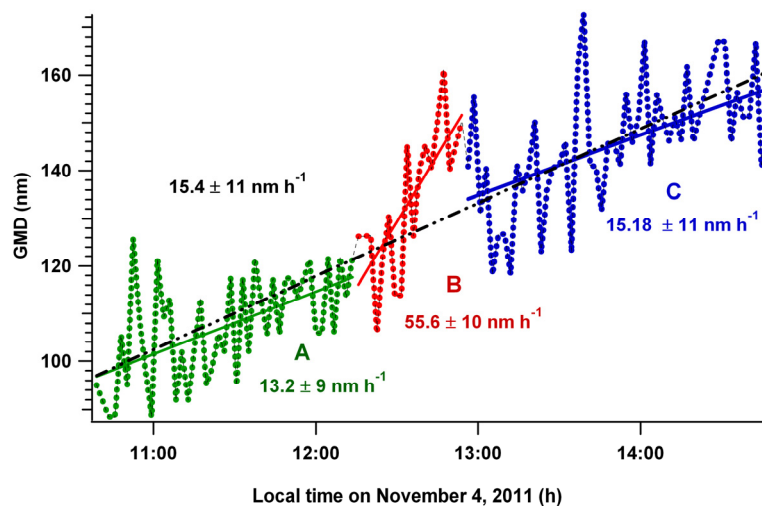


**Fig. 7.** A plot between the geometric mean diameter (GMD) versus local time on a growth event day for calculation of particle growth rates using slope of regression fit. The standard error shown with growth rate is computed as an error of the regression fit for the predicted growth rate.

shows a positive correlation ( $r^2 = 0.30$ ), whereas solar radiation exhibits a strong negative correlation ( $r^2 = -0.74$ ) with  $GR_{\text{scav}}$  (this point is further discussed in the following section). Other possible reason may be the  $GR_{\text{scav}}$  is overwhelmed by the growth rate due to coagulation scavenging ( $GR_{\text{scav}}$ ), especially during noontime when solar radiation and temperature are intensified (opposite

characteristic to the  $GR_{\text{scav}}$ ).

The  $GR_{\text{scav}}$  was calculated using Eq. (10). In this study (on November 4), we did not observe any mode peak in nucleation range (< 25 nm). As discussed in Fig. 4, we assumed that the nucleation range particles in the primary size distribution are being scavenged by mode peak particles existing in the same distribution, which results in to the next

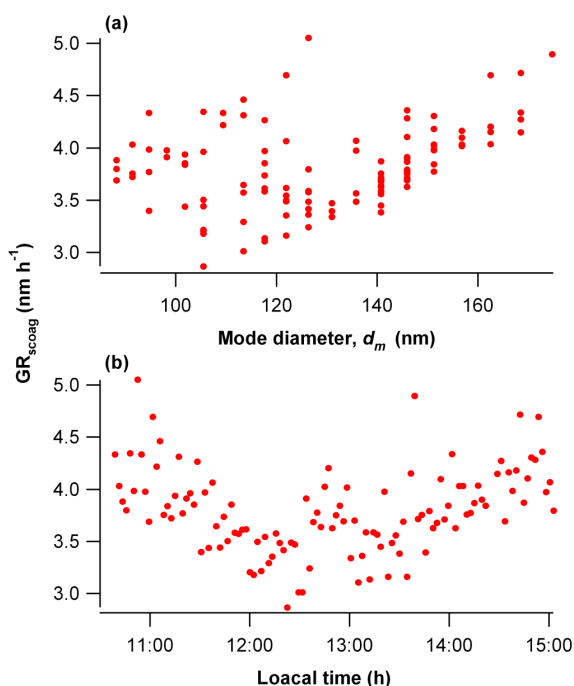


**Fig. 8.** The relation between (a) calculated  $GR_{scog}$  using Eq. (4) and particle mode size distribution, (b)  $GR_{scog}$  and local time on November 4.

mode in the succeeding sample. The average growth rate ( $GR_{scav}$ ) was calculated to be  $8.0 \pm 6$  nm/h with minimum and maximum values of 0.6 and 19.3 nm/h, respectively.

Here it is important to note that the mode peak may shift in several conditions, which include: (i) If particles exist in the same mode peak will coagulate (i.e., self-coagulation) and thus mode peak will shift in the succeeding sample, but number concentration of mode peak particles will decrease continuously in the successive measurements. This was observed in this study, Fig. 5(a). (ii) When nucleation range particles will scavenge by mode peak particles. In this case number concentration of mode peak will not be affected but peak will shift (a case of coagulation scavenging, e.g., Fig. 4). (iii) The growth observed in this study is based on the particle distribution measured for  $< 425$  nm. However, according to the polydisperse coagulation theory, the coagulation proceeds faster as the size difference between two particles becomes larger. Therefore in the atmosphere, the mode peak particles may be scavenged by bigger particles (i.e.,  $> 425$  nm). This effect is not accounted in this study. However, if this effect is considerable then it may only affect the mode peak particle number concentration, but will not affect the mode peak shifting (particle growth) in the size range which is being studied here.

Fig. 9(a) shows an increasing trend of  $GR_{scav}$  with respect to local time. This may relate with meteorological condition.  $GR_{scav}$  is positively correlated with meteorological parameters, e.g., temperature ( $r^2 = 0.83$ ), wind speed ( $r^2 = 0.62$ ) and solar radiation ( $r^2 = 0.28$ ), whereas negatively correlated with relative humidity ( $r^2 = -0.21$ ). These characteristics of  $GR_{scav}$  are observed to be opposite to that of  $GR_{scog}$ . A possible reason for a good relation of  $GR_{scav}$

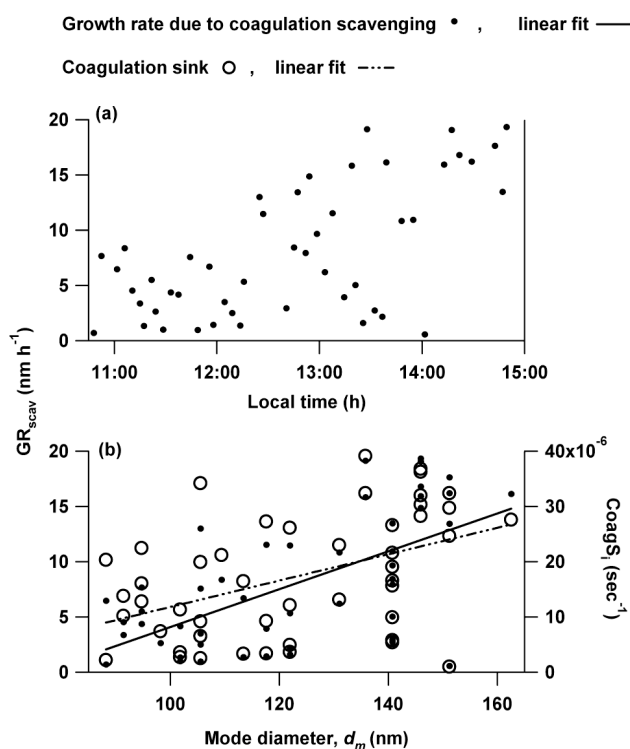


**Fig. 9.** The relationship between (a) growth rate due to coagulation scavenging ( $GR_{scav}$ ) and local time, (b) ( $GR_{scav}$ ) and mode diameter ( $d_m$ ), and coagulation sink and  $d_m$ .

with temperature and wind speed could be that the high temperature leads to intensify the Brownian collision and low wind speed creates favorable condition for the coagulation scavenging of particles (this point is further discussed in the following section).

The coagulation sink is calculated using Eqs. (6)–(8). Similar to  $GR_{scav}$ , the coagulation sink is also showed increasing trend with particle mode peak diameter (Fig. 9(b)). The correlations of  $GR_{scav}$  with particle mode peak diameter ( $d_m$ ), and coagulation sink with  $d_m$  are calculated to be  $r^2 = 0.62$  and  $r^2 = 0.45$ , respectively. This suggests that particles of larger diameter can act as better sink and grow by scavenging of increased number of newly formed nucleation range particles ( $< 12$  nm in this case).

Growth rate due to condensation was calculated ( $GR_{cond}$ ) using Eq. (3), where we input  $GR_{total}$ ,  $GR_{scog}$  and  $GR_{scav}$  values (average), and thus  $GR_{cond}$  retrieved to be 3.6 nm/h. Using condensational growth rate one can determine the concentration of condensable vapors using Eq. (11).

#### **Effect of Meteorological Parameters on Particle Growth**

Apart from concentration of precursor species in the atmosphere, the meteorological conditions play an important role in the new particle formation and its successive growth. Fig. 10 illustrates the effect of meteorological parameters on the particle growth event and non-event days. Fig. 10(a) clearly shows that the temperature (30 min average) is higher on growth event day than that of non-event day. Also the variation between minimum and maximum temperature is relatively larger on event day. During noontime (12:00–

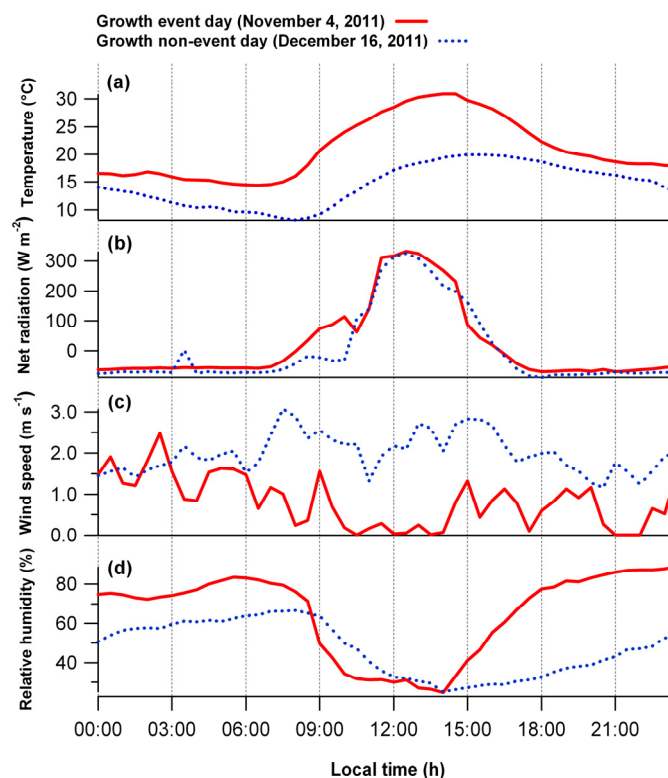


**Fig. 10.** Meteorological parameters on particle growth event and non-event days.

15:00 h) on November 4 where the temperature is peaked, the dominant process of growth in this study, i.e., coagulation scavenging is also maximized (as discussed above). Although temperature is higher for event day, interestingly solar radiation was almost the same for event day and non-event day, Fig. 10(b). This suggests that high temperature condition favors the particle growth, and on the other hand, similar solar radiation condition on event and non-event days possibly indicating that precursor species are also important directly/indirectly for formation and growth of particles. Precursor gas species possibly absorbs heat and therefore enhance the temperature at the ground level, while particles (especially fresh secondary aerosols) may scatter solar radiation resulting to reduce the solar radiation at the surface. It is important to note that the observed diurnal temperature behavior is quite different from clean areas, as recorded at different locations in Finland (Boy and Kulmala, 2002; Komppula *et al.*, 2003; Vehkamäki *et al.*, 2004), where it has been found that the average temperatures for event days were lower than that of non-events days. Contrarily, high temperature conditions have been found to be associated with the nucleation events and subsequent growth in east and south Germany (Birmili and Wiedensohler, 2000; Birmili *et al.*, 2003), and in Atlanta (Woo *et al.*, 2001).

Observing the high solar radiation during event days than non-event days has been the main feature found in all long-term nucleation and growth studies from clean areas in Finland (Mäkelä *et al.*, 1997; Kulmala *et al.*, 1998; Boy and Kulmala, 2002; Komppula *et al.*, 2003; Vehkamäki *et al.*, 2004) to industrial and agriculture regions in Germany (Birmili and Wiedensohler, 2000; Birmili *et al.*, 2003),

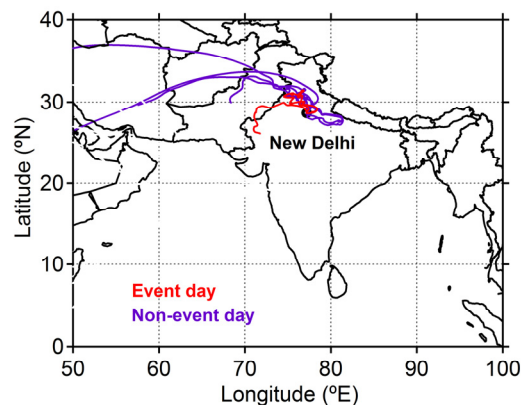
Birmingham, UK (Alam *et al.*, 2003), Pittsburgh, Pennsylvania (Stanier *et al.*, 2004), urban Atlanta (Woo *et al.*, 2001) and rural environment in north Italy (Rodriguez *et al.*, 2005). These studies concluded that photochemistry is a governing process which involves formation of the hydroxyl radical (Harrison *et al.*, 2000) and thus produces the nucleating and/or condensing species for the new particle formation and subsequent growth.

Fig. 10(c) shows that wind speed was on average lower on growth event day than on growth non-event day. During the growth period on November 4, the observed average wind speed was 0.6 m/s, whereas for the same period on December 16, the recorded value was 2.3 m/s. This suggests that high temperature and calm conditions support the particle growth, especially growth due to coagulation scavenging as discussed above. In above discussions, it was observed that relative humidity is negatively ( $r^2 = -0.21$ ) and positively ( $r^2 = 0.30$ ) correlated with growth rates due to coagulation scavenging ( $GR_{scav}$ ) and self-coagulation ( $GR_{scoag}$ ), respectively. The coagulation scavenging was found as dominant process for growth on November 4. On comparing the effect of relative humidity during growth period and for the same period on non-event day in Fig. 10(d), no remarkable difference was observed. Different behavior was observed in north Italy (Rodriguez *et al.*, 2005), in the polluted continental boundary layer (Birmili and Wiedensohler, 2000), in rural area (Birmili *et al.*, 2003) and also in clean areas, for example in different stations in Finland, i.e., Hyytiälä station (Boy and Kulmala, 2002), Pallas station in sub arctic area in northern Finland (Komppula *et al.*, 2003) and in Väriö in Finnish Lapland

(Vehkamäki *et al.*, 2004). Where it was observed that the particle formation and growth are negatively correlated with relative humidity, consistent with this study in the case of growth due to coagulation scavenging. Further, the slope in Fig. 7 is abruptly changed during noontime (12:00–13:00 h), i.e., regression line B, which is possibly because of increase of temperature and low wind speed conditions. These conditions favor and enhance the photochemical secondary growth (condensation) rate.  $GR_{\text{cond}}$  for three different slopes, A, B and C are retrieved to be 5.4, 42.3 and - (no growth) nm/h, respectively (whereas  $GR_{\text{scav}}$ , and  $GR_{\text{scav}}$  for these slopes are calculated to be 4.0, 9.7 and 11.5 nm/h, and 3.8, 3.6 and 3.8 nm/h, respectively).

The observed growth rates on other two event days, i.e., on December 15 and 26, 2011 were  $13.37 \pm 12$  nm/h and  $9.5 \pm 10$  nm/h, respectively. The minimum particle number concentration was  $1.1 \times 10^4$  and maximum was  $3.2 \times 10^4$  particle/cm<sup>3</sup> on December 15. Whereas on December 26, these concentrations were  $2.4 \times 10^4$  and  $3.5 \times 10^5$  particle/cm<sup>3</sup>, respectively. The estimated self-coagulation growth rate ( $GR_{\text{scav}}$ ) for both the event days were  $2.0 \pm 0.5$  and  $4.0 \pm 2$  nm/h, respectively. Similar to November 4, the correlation of meteorological data with  $GR_{\text{scav}}$  of other two event days (December 15 and 26) were also studied. Relative humidity of both the event days shows strong positive correlation with self-coagulation growth rate, i.e.,  $r^2 = 0.96$  and  $0.92$ , respectively. Whereas, temperature ( $r^2 = -0.95$  and  $-0.88$ ), wind speed ( $r^2 = -0.86$  and  $-0.57$ ) and solar radiation ( $r^2 = -0.63$  and  $-0.68$ ) shows negative correlations with  $GR_{\text{scav}}$  on both the event days, respectively. Unlike November 4, the growth rate due to scavenging was not estimated for these events because of the absence of particle number concentration of below 12 nm (< 12 nm assumed to be freshly formed in this study as discussed above (10 nm assumed by Kulmala *et al.*, 2000)).

Five-day air mass backward trajectories were obtained for each of the measurement days. The analysis was performed using the HYSPLIT-WEB model (<http://ready.arl.noaa.gov/HYSPLIT.php>, NOAA Air Resources Laboratory, Silver Spring, Maryland, United States). These trajectories were calculated for air masses starting from the sampling site (with sampling ending time) at 500 m height using the model vertical velocity and reanalysis data. The flow pattern was updated every 24 h. During 10 days of the measurement, 3 growth event days were identified. In Fig. 11, the backward trajectories clearly show that during growth event days (red inked), air masses were relatively fresh and arrived to the site from western side compared to those for non-event days, where air masses were traveled longer distances (aged) and/or originated from Indo-Gangetic plain (blue inked). Aerosols in Indo-Gangetic plain are reported to be aged because of poor ventilation in this plain. This analysis also suggests that in New Delhi, formation and growth of aerosols (secondary aerosols) and air quality possibly influenced by the regional emission inflow in addition to local emission sources, e.g., biomass burning, traffic emission, biogenic emission and other combustion/burning sources from residential colonies (Miyazaki *et al.*, 2009; Li *et al.*, 2014).



**Fig. 11.** Five-day backward trajectories obtained for each of the measurement days (<http://ready.arl.noaa.gov/HYSPLIT.php>, NOAA Air Resources Laboratory, Silver Spring, Maryland, United States).

## CONCLUSION

For different purposes in atmospheric aerosol studies, information on particle growth due to individual process is needed. In this study, based on the equations discussed in Leppä *et al.* (2011), we applied a simplified approach to calculate particle growth due to self-coagulation, coagulation scavenging and condensation (Seinfeld and Pandis, 2006) processes. This approach is based on particle number size distribution measured by SMPS. The SMPS measurements (particle size range from 9–425 nm) were conducted at National Physical Laboratory, New Delhi for 10 days during November–December 2011. In this period, 3 particle growth event days were classified. To discuss growth rate due to self-coagulation ( $GR_{\text{scav}}$ ), coagulation scavenging ( $GR_{\text{scav}}$ ) and condensation ( $GR_{\text{cond}}$ ) using the formulae derived in this study, for an example, we have selected a growth event day, November 4 and a non-event day, December 16. Total growth rate ( $GR_{\text{total}}$ ) was calculated based on the regression fit of the plot between geometric mean diameter (GMD) and local time of the number size distribution measured on November 4. From the regression equation,  $GR_{\text{total}}$  calculated to be  $15.4 \pm 11$  nm/h. Using the formulae derived in this study,  $GR_{\text{scav}}$  and  $GR_{\text{scav}}$  were calculated to be  $3.8 \pm 0.4$  and  $8.0 \pm 6$  nm/h, respectively. Assuming that the total growth rate is a sum of  $GR_{\text{scav}}$ ,  $GR_{\text{scav}}$  and  $GR_{\text{cond}}$ ,  $GR_{\text{cond}}$  is estimated to be 3.6 nm/h. This approach is simple, and growth by individual processes can be calculated without knowing several other parameters which include vapor concentration of atmospheric constituents, heterogeneous processes, complex modeling procedures, etc.

Our result suggests that (i) on an event day (November 4), particle mode peak size is increased with time but number concentration in the mode is systematically decreased. Furthermore, particle total number concentration is also found to decrease with particle mode peak size. This suggests that coagulation scavenging is a dominant process of particle growth in an urban atmosphere, (ii) the  $GR_{\text{scav}}$  was found to be relatively low around noontime, when solar radiation is peaked ( $r^2 = -0.74$ ) and relative humidity

is low ( $r^2 = 0.30$ ), (iii) on the other hand, different from  $GR_{\text{scog}}$ ,  $GR_{\text{scav}}$  exhibits opposite characteristics. The  $GR_{\text{scav}}$  is positively correlated with temperature ( $r^2 = 0.83$ ), wind speed ( $r^2 = 0.62$ ) and solar radiation ( $r^2 = 0.28$ ), whereas, negatively correlated with relative humidity ( $r^2 = -0.21$ ), (iv) like  $GR_{\text{scav}}$ , the coagulation sink is also showed increased trend with particle mode peak diameter. This suggests that particles of larger diameter can act as better sink and grow by scavenging of increased number of newly formed nucleation range particles ( $< 12$  nm in this case). Further studies are needed to fully understand these mechanisms in the atmosphere.

The total growth rate observed in New Delhi is comparable with the growth rates observed in several sites on the globe those are affected by long-range anthropogenic transport, local traffic, industrial and biomass burning emissions. This supports the reported increased level of emissions in the megacity.

## ACKNOWLEDGEMENTS

BS is thankful to Department of Science and Technology, New Delhi for awarding INSPIRE research fellowship. We gratefully acknowledge Prof. R.C. Budhani, Director, CSIR-NPL for providing facility for this work. We thank two anonymous reviewers for the valuable comments and suggestions.

## REFERENCES

- Aggarwal, S.G., Sarangi, B., Kumar, S. and Gupta, P.K. (2013). A Simplified Approach to calibrate Condensation Particle Counter for Aerosol Number Concentration Measurement, 8th International Conference on Advances in Metrology (AdMet-2013) and Pre-AdMet Workshop, February 20–23, 2013, New Delhi, India, OP-26, P100-101.
- Alam, A., Shi, J.P. and Harrison, R.M. (2003). Observations of New Particle Formation in Urban Air. *J. Geophys. Res.* 108: 4093, doi: 10.1029/2001JD001417.
- Allen, M.D. and Raabe, O.G. (1985). Slip Correction Measurements of Spherical Solid Aerosol Particles in an Improved Millikan Apparatus. *Aerosol Sci. Technol.* 4: 269–286.
- Asmi, E., Frey, A., Virkkula, A., Ehn, M., Manninen, H.E., Timonen, H., Tolonen-Kivimäki O., Aurela, M., Hillamo, R. and Kulmala, M. (2010). Hygroscopicity and Chemical Composition of Antarctic sub-micrometre Aerosol Particles and observations of New Particle Formation. *Atmos. Chem. Phys.* 10: 4253–4271.
- Birmili, W. and Wiedensohler, A. (2000). New Particle Formation in the Continental Boundary Layer: Meteorological and Gas Phase Parameter Influence. *Geophys. Res. Lett.* 27: 3325–3328.
- Birmili, W., Berresheim, H., Plass-Dülmer, C., Elste, T., Gilge, S., Wiedensohler, A. and Uhrner, U. (2003). The Hohenpeissenberg Aerosol Formation Experiment (HAFEX): A Long-term Study Including Size-resolved Aerosol,  $H_2SO_4$ , OH, and Monoterpenes Measurements. *Atmos. Chem. Phys.* 3: 361–376.
- Boy, M. and Kulmala, M. (2002). Nucleation Events in the Continental Boundary Layer: Influence of Physical and Meteorological Parameters. *Atmos. Chem. Phys.* 2: 1–16.
- Butler, T., Denier van der Gon, H.A.C. and Kuenen, J. (2011). The Base Year (2005) Global Gridded Emission Inventory Used in the EU FP7Project MEGAPOLI (Final Version). MEGAPOLI Scientific Report 11-02, MEGAPOLI-28-REP-2011-01, 27p, ISBN: 978-87-92731-06-7.
- Bzdek, B.R. and Johnston, M.V. (2010). New Particle Formation and Growth in the Troposphere. *Anal. Chem.* 82: 7871–7878.
- Cheung, H.C., Morawska, L. and Ristovski, Z.D. (2011). Observation of New Particle Formation in Subtropical Urban Environment. *Atmos. Chem. Phys.* 11: 3823–3833, doi: 10.5194/acp-11-3823-2011.
- Coakley, J. (2005). Reflections on Aerosol Cooling. *Nature* 438: 1091–1092.
- Dal Maso, M., Kulmala, M., Riipinen, I., Wagner, R., Hussein, T., Aalto, P.P. and Lehtinen, K.E.J. (2005). Formation and Growth of Fresh Atmospheric Aerosols: Eight Years of Aerosol Size Distribution Data from SMEAR II, Hyytiälä, Finland. *Boreal Environ. Res.* 10: 323–336.
- Dal Maso, M., Sogacheva, L., Aalto, P.P., Riipinen, I., Komppula, M., Tunved, P., Korhonen, L., Suur-Uski, V., Hirsikko, A., Kurt'ën, T., Kerminen, V.M., Lihavainen, H., Viisanen, Y., Hansson, H.C. and Kulmala, M. (2007). Aerosol Size Distribution Measurements at Four Nordic Field Stations: Identification, Analysis and Trajectory Analysis of New Particle Formation Bursts. *Tellus Ser. B* 59: 350–361.
- Du, J., Cheng, T., Zhang, M., Chen, J., He, Q., Wang, X., Zhang, R., Tao, J., Huang, G., Li, X. and Zha, S. (2012). Aerosol Size Spectra and Particle Formation Events at Urban Shanghai in Eastern China. *Aerosol Air Qual. Res.* 12: 1362–1372.
- Finlayson-Pitts, B.J. and Pitts Jr., J.N. (2000). *Chemistry of the Upper and Lower Atmosphere*, Academic Press, San Diego.
- Fuchs, N.A. (1964). *The Mechanics of Aerosols*, Pergamon Press, Oxford, UK.
- Hamed, A., Joutsensaari, J., Mikkonen, S., Sogacheva, L., Dal Maso, M., Kulmala, M., Cavalli, F., Fuzzi, S., Facchini, M.C., Decesari, S., Mircea, M., Lehtinen, K.E.J. and Laaksonen, A. (2007). Nucleation and Growth of New Particles in Po Valley, Italy. *Atmos. Chem. Phys.* 7: 355–376.
- Han, Y., Iwamoto, Y., Nakayama, T., Kawamura, K., Hussein, T. and Mochida, M. (2013). Observation of New Particle Formation over A mid-latitude Forest Facing the North Pacific. *Atmos. Environ.* 64: 77–84.
- Harrison, R.M., Grenfell, J.L., Savagen, N., Allen, A., Clemit-shaw, K.C., Penkett, S., Hewitt, C.N. and Davison, B. (2000). Observations of New Particle Production in the Atmosphere of a Moderate Polluted Site in Eastern England. *J. Geophys. Res.* 105: 17819–17832.
- Hinds, W.C. (1998). *Aerosol Technology: Properties, Behaviour, and Measurement of Airborne Particles*,

- Second Edition, John Wiley & Sons, Inc., USA.
- Hirsikko, A., Vakkari, V., Tiitta, P., Manninen, H.E., Gagné, S., Laakso, H., Kulmala M., Mirme, A., Mirme, S., Mabaso D., Beukes, J.P. and Laakso, L. (2012). Characterisation of Sub-micron Particle Number Concentrations and Formation Events in the Western Bushveld Igneous Complex, South Africa. *Atmos. Chem. Phys.* 12: 3951–3967.
- Jacobson, M.Z. and Turco, R. (1994). Modeling Coagulation among Particles of Different Composition and Size. *Atmos. Environ.* 28: 1327–1338.
- Jeong, C.H., Evans, G.J., McGuire, M.L., Chang, R.Y.-W., Abbatt, J.P.D., Zeromskiene, K., Mozurkewich, M., Li, S.M. and Leitch, W.R. (2010). Particle Formation and Growth at Five Rural and 20 Urban Sites. *Atmos. Chem. Phys.* 10: 7979–7995, doi: 10.5194/acp-10-7979-2010.
- Kalafut-Pettibone, A.J., Wang, J., Eichinger, W.E., Clarke, A., Vay, S.A., Blake, D.R. and Stanier, C.O. (2010). Size-resolved Aerosol Emission Factors and New Particle Formation/Growth Activity Occurring in Mexico City during the MILAGRO 2006 Campaign. *Atmos. Chem. Phys.* 11: 8861–8881.
- Kaufman, Y.J. and Koren, I. (2006). Smoke and Pollution Aerosol Effect on Cloud cover. *Science* 313: 655–658.
- Kerminen, V.M., Anttila, T., Petäjä, T., Laakso, L., Gagné, S., Lehtinen, K.E.J. and Kulmala, M. (2007). Charging State of the Atmospheric Nucleation Mode: Implications for Separating Neutral and Ion-induced Nucleation. *J. Geophys. Res.* 112, D21205, doi: 10.1029/2007JD008649.
- Kim, Y.P. and Seinfeld, J.H. (1990). Numerical Solution of the Multicomponent Aerosol General Dynamic Equation, Proceeding 3rd. Int. Aerosol Conference, Science, Industry, Health and Environment, Pergamon Press, Oxford.
- Komppula, M., Dal Maso, M., Lihavainen, H., Aalto, P.P., Kulmala, M. and Viisanen, Y. (2003). Comparison of New Particle Formation Events at Two Locations in Northern Finland. *Boreal Environ. Res.* 8: 395–404.
- Kuang, C., Chen, M., Zhao, J., Smith, J., McMurry, P.H. and Wang, J. (2012). Size and Time-resolved growth Rate Measurements of 1 to 5 nm Freshly Formed Atmospheric Nuclei. *Atmos. Chem. Phys.* 12: 3573–3589, doi: 10.5194/acp-12-3573-2012.
- Kulmala, M., Toivonen, A., Mäkelä, J.M. and Laaksonen, A. (1998). Analysis of the Growth of Nucleation Mode Particles Observed in Boreal Forest. *Tellus Ser. B* 50: 449–462.
- Kulmala, M., Pirjola, L. and Mäkelä, J.M. (2000). Stable Sulphate Clusters as a Source of New Atmospheric Particles. *Nature* 404: 66–69.
- Kulmala, M., Dal Maso, M., Mäkelä, J.M., Pirjola, L., Väkevä, M., Aalto, P., Miikkulainen, P., Hämeri, K. and O'Dowd, C. (2001). On the Formation, Growth and Composition of Nucleation Mode Particles. *Tellus Ser. B* 53: 479–490.
- Kulmala, M., Vehkamäki, H., Petäjä, T., Dal Maso, M., Lauri, A., Kerminen, V.M.W., Birmili, W. and McMurry, P.H. (2004). Formation and Growth Rates of Ultrafine Atmospheric Particles: A Review of Observations. *J. Aerosol Sci.* 35: 143–176.
- Kulmala, M., Petäjä, T., Mönkkönen, P., Koponen, I.K., Dal Maso, M., Aalto, P.P., Lehtinen, K.E.J. and Kerminen, V.M. (2005). On the Growth of nucleation Mode Particles: Source Rates of Condensable Vapor in Polluted and Clean Environments. *Atmos. Chem. Phys.* 5: 409–416.
- Kulmala, M., Kontkanen, J., Junninen, H., Lehtipalo, K., Hanna, E., Manninen, Nieminen, T., Petäjä, T., Sipilä, M., Schobesberger, S., Rantala, P., Franchin, A., Jokinen, T., Järvinen, E., Äijälä, M., Kangasluoma, J., Hakala, J., Aalto, P., Paasonen, P., Mikkilä, J., Vanhanen, J., Aalto, J., Hakola, H., Makkonen, U., Ruuskanen, T., Mauldin III, R.L., Duplissy, J., Vehkamäki, H., Bäck, J., Kortelainen, A., Riipinen, I., Kurtén, T., Johnston, M.V., Smith, J.N., Ehn, M., Mentel, T.F., Lehtinen, K.E.J., Laaksonen, A., Kerminen, V.M. and Worsnop, D.R. (2013). Direct Observations of Atmospheric Aerosol Nucleation. *Science* 339: 943; doi: 10.1126/science.1227385
- Laaksonen, A., Hamed, A., Joutsensaari, J., Hiltunen, L., Cavalli, F., Junkermann, W., Asmi, A., Fuzzi, S. and Facchini, M.C. (2005). Cloud Condensation Nucleus Production from Nucleation Events at a Highly Polluted Region. *Geophys. Res. Lett.* 32: L06812, doi: 10.1029/2004GL022092.
- Lehtinen, K.E.J. and Kulmala, M. (2003). A Model for Particle Formation and Growth in the Atmosphere with Molecular Resolution in Size. *Atmos. Chem. Phys.* 3: 251–257.
- Leppä, J., Anttila, T., Kerminen, V.M., Kulmala, M. and Lehtinen, K.E.J. (2011). Atmospheric New Particle Formation: Real and Apparent Growth of neutral and Charged Particles. *Atmos. Chem. Phys.* 11: 4939–4955.
- Li, J., Wang, G., Aggarwal, S.G., Huang, Y., Ren, Y., Zhou, B., Singh, K., Gupta, P.K., Cao, J. and Zhang, R. (2014). Comparison of Abundances, Compositions and Sources of Elements, Inorganic Ions and Organic Compounds in Atmospheric Aerosols from Xi'an and New Delhi, Two Megacities in China and India. *Sci. Total Environ.* 476–477: 485–495.
- Mäkelä, J.M., Aalto, P., Jokinen, V., Pohja, T., Nissinen, A., Palmroth, S., Markkanen, T., Seitsonen, K., Lihavainen, H. and Kulmala, M. (1997). Observations of Ultrafine Aerosol Particle Formation and Growth in Boreal Forest. *Geophys. Res. Lett.* 24: 1219–1222.
- Mäkelä, J.M., Dal Maso, M., Pirjola, L., Keronen, P., Laakso, L., Kulmala, M. and Laaksonen, A. (2000). Characteristics of the Atmospheric Particle Formation Events Observed at A Boreal Forest site in Southern Finland. *Boreal Environ. Res.* 5: 299–313.
- Miyazaki, Y., Aggarwal, S.G., Singh, K., Gupta, P.K. and Kawamura, K. (2009). Dicarboxylic Acids and Water-soluble Organic Carbon in Aerosols in New Delhi, India in Winter: Characteristics and Formation Processes. *J. Geophys. Res.* 114, doi: 10.1029/2009JD011790.
- Mochida, M., Miyakawa, T., Takegawa, N., Morino, Y., Kawamura, K. and Kondo, Y. (2008). Significant Alteration in the Hygroscopic Properties of Urban Aerosol Particles by the Secondary Formation of Organics.

- Geophys. Res. Lett.* 35: L02804, doi: 10.1029/2007GL031310.
- Nieminen, T., Lehtinen, K.E.J. and Kulmala, M. (2010). Sub-10 nm Particle Growth by Vapor Condensation – Effects of Vapor Molecule Size and Particle Thermal Speed. *Atmos. Chem. Phys.* 10: 9773–9779, doi: 10.5194/acp-10-9773-2010.
- Pirjola, L., O’Dowd, C.D. and Kulmala, M. (2002). A Model Prediction of the Yield of Cloud Condensation Nuclei from Coastal Nucleation Events. *J. Geophys. Res.* 107: 8098, doi: 10.1029/2000JD000213.
- Rodriguez, S., Van Dingenen, R., Putaud, J.P., Martins-Dos Santos, S. and Roselli, D. (2005). Nucleation and Growth of New Particles in the Rural Atmosphere of Northern Italy -relationship to Air Quality Monitoring. *Atmos. Environ.* 39: 6734–6746.
- Seinfeld, J.H. and Pandis, S.N. (2006). *Atmospheric Chemistry and Physics: From Air Pollution to Climate Change*, Second Edition, John Wiley & Sons, Inc., New Jersey.
- Stanier, C.O., Khlystov, A.Y. and Pandis, S.N. (2004). Nucleation Events during the Pittsburgh Air Quality Study: Description and Relation to Key Meteorological, Gas Phase, and aerosol Parameters. *Aerosol Sci. Technol.* 38: 253–264.
- Turco, R.P., Hamill, P., Toon, O.B., Whitten, R.C. and Kiang, C.S.J. (1979). The NASA - Ames Research Center Stratospheric Aerosol Model: Physical Processes and Computational Analogs, NASA Technical Publication.
- Twomey, S. (1974). Pollution and Planetary Albedo. *Atmos. Environ.* 8: 1251–1256.
- Vehkamäki, H., Dal Maso, M., Hussein, T., Flanagan, R., Hyvärinen, A., Lauros, J., Merikanto, J.P., Mönkkönen, P., Pihlatie, M., Salminen, K., Sogacheva, L., Thum, T., Ruuskanen, T.M., Keronen, P., Aalto, P.P., Hari, P., Lehtinen, K.E.J., Rannik, Ü. and Kulmala, M. (2004). Atmospheric Particle Formation Events at Värriömeasurement Station in Finnish Lapland 1998–2002. *Atmos. Chem. Phys.* 4: 2015–2023.
- Verheggen, B. and Mozurkewich, M. (2002). Determination of Nucleation and Growth Rates from Observation of a SO<sub>2</sub> Induced Atmospheric Nucleation Event. *J. Geophys. Res.* 107: 4123, doi: 10.1029/2001JD000683.
- Wang, L., Khalizov, A. F., Zheng, J., Xu, W., Ma, Y., Lal, V. and Zhang, R. (2010). Atmospheric Nanoparticles Formed from Heterogeneous Reactions of Organics. *Nat. Geosci.* 3: 238–242, doi: 10.1038/ngeo778.
- Weber, R.J., Marti, J.J., McMurry, P.H., Eisele, F.L., Tanner, D.J. and Jefferson, A. (1997). Measurements of New Particle Formation and Ultrafine Particle Growth Rates at a Clean Continental Site. *J. Geophys. Res.* D102: 4375–4385.
- Woo, K.S., Chen, D.R., Pui, D.Y.H. and McMurry, P. H. (2001). Measurement of Atlanta Aerosol Size Distributions: Observations of Ultrafine Particle Events. *Aerosol Sci. Technol.* 34: 75–87.
- Zhang, Y.M., Zhang, X.Y., Sun, J.Y., Lin, W.L., Gong, S. L., Shen, X.J. and Yang, S. (2011). Characterization of New Particle and Secondary Aerosol Formation during Summertime in Beijing, China. *Tellus Ser. B* 63: 382–394.

Received for review, December 14, 2013

Revised, February 23, 2014

Accepted, April 13, 2014